EUROPEAN ORGANIZATION FOR NUCLEAR RESEARCH
CERN - SL Division

SL / Note 95 - 06 (BT)

ANALYSIS OF THE INDUCED RADIOACTIVITY IN THE SPS EXTRACTION CHANNELS DURING 1994

F. Ferioli, R.L.Keizer

Geneva, Switzerland
December 1994

Page of contents

Summary

The induced radioactivity (IR) caused by beam loss in the CERN SPS extraction channel in LSS6, has been monitored during 1994 with six BLX ionization monitors equipped with special high gain amplifiers. The aim of this experiment was to explore the possibility of detecting hot spots in real time and calculating the decay time given the time function of daily extracted number of protons. This report describes the experience gained during six months of operation.

1 INTRODUCTION

The quality of the setting-up during the extraction of protons from the SPS is of crucial importance for the survival of the equipment and safety of the personnel.

One of the relevant phenomnea is the formation of hot-spots indicating that something has ran out of control and the beam has strongly activated a particular piece of equipment. Up to now these hot-spots were measured during the shut-down, a long time after the moment that proper corrective action should have been undertaken.

The measurement of the instantaneous induced radioactivity (IR) allows very quick detection of hot-spots and provides instantaneous feed-back to the operations-crew.

Another aspect of the operation and maintenance of extraction channels is the exact time-dependance of the radioactive decay curve which in turn determines the waiting time for access to the equipment. It would be useful to calculate this curve for each point of the extraction channel from the number of daily extracted protons.

During the 1993/94 shut-down the five BLX ionization monitors in LSS6 were repositioned, a new one was added and the ensemble was prepared to measure the induced activity.

A by-product of this research was the discovery that also micro beam losses during injection and acceleration of protons and leptons could be measured.

2 MEASUREMENT OF THE INDUCED RADIOACTIVITY

2.1 Acquisition, layout and method.

1993. The 1993 measurements were carried out with 5 ionization monitors equipped with high-gain amplifiers, installed in LSS6, namely 61634, 61636, 61833, 61835 and 61874. These had previously had been used for p-pbar operation. It turned out to be possible to measure the induced radioactivity during the quiet part of the 14.4 s machine cycle, namely when the protons have left the machine. The technical problem is that the electronics should have a quick recovery-time because, during the extraction, the flux of secondary particles causes a strong signal, roughly three to four orders of magnitude larger than the IR, causing strong saturation.

1994. During the 1993/94 shut-down 6 ionization monitors were installed and relocated at well defined positions, namely 61636 (ZS1), 61680 (ZS5), 61775 (MST1), 61796 (MST3), 61833 (MSE1) and 61874 (MSE5).

Table 1 gives the integration periods which were used.

acquisition	action	time [ms]	interval [ms]	event code	definition
1	start	7360		21290101	f/s2 stop
	stop	8629	1269	21550301	
2	start	8800		21430101	
	stop	9690	890	21200301	e^+1 inj. warning
3	start	10150		21270301	e^+1 extr. stop
	stop	10890	740	21200302	e^+2 inj. warning
4	start	11350		21270302	e^+2 extr. stop
	stop	12090	740	21200401	e^-1 inj. warning
5	start	12550		21270401	e^-1 extr. stop
	stop	13290	740	21200402	e^-2 inj. warning
6	start	13750		21270402	e^-2 extr. stop
	stop	14340	590	21200101	p1 inj. warning
7	start	40		21210101	
	stop	1140	1100	21220101	

Table 1 Event code table

The beam monitor integral is generated by integrating the ionization counter output during the interval under consideration.

The IR is defined as the increase of beam monitor integral per unit time, arbitrarily expressed in bits per s.

1994-08-05-09:17:46
RADIATION EN BIT/S GAIN 1*100

TIME	ZS1	ZS5	TPSN	MST3	MSE1	MSE5
	61636	61680	61775	61796	61833	61874
7360	598	5169	974	407	233	152
8800	375	2484	502	217	128	82
10150	275	1352	295	130	84	51
11350	226	852	196	83	61	37
12550	203	622	151	66	54	30
13750	190	509	131	54	48	25
40	191	491	126	80	174	33

Table 2 Typical set of acquired parameters

A typical set of data is shown in Table 2. The first 6 measurements are made during a particular machine cycle. The last measurement is made during the following cycle. The latter period, as Table 1 shows, coincides with the two-batch proton injection.

The indicated TIME is the beginning of the period [ms]. Table 1 gives the length of each period. The figures which follow represent the IR.

If there are small proton injection losses these reveal themselves by an increase of the signal strength. This happened to be the case because MST3, MSE1 and MSE5 indicate additional beamloss. For MSE1 the increase of 126 arbitrary units is equivalent to some 1% of the extraction loss. No such beamloss has been seen in LSS2.

It also happens that sometimes losses occur during lepton acceleration, measurements 4 and 5. The signal therefore increases.

For exact IR measurement these conditions, leading to a false interpretation, should be avoided.

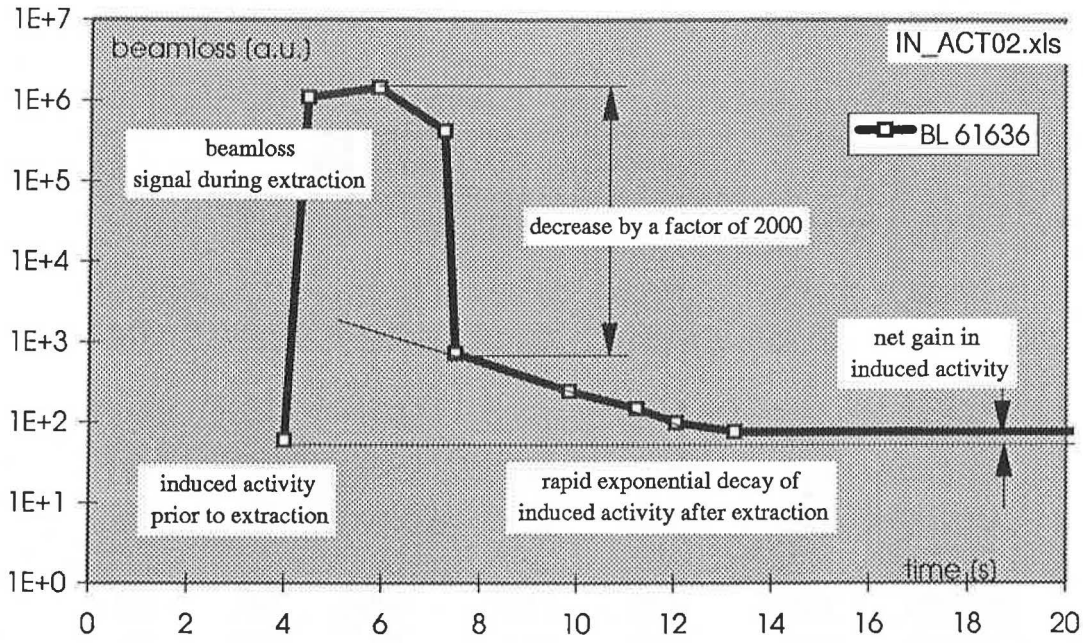

Fig 1 Activation and exponential decay

An example of activation during extraction followed by rapid exponential decay is shown in fig 1. The beamloss signal is 2000 times stronger than the subsequent induced activity signal. In this particular case there was a net gain of induced activity after one machine cycle. The points of the next cycle which sustantiate this small increase are not shown.

Other measurements during each start-up, not shown here, show that temporary equilibrium is reached after only a few machine cycles.

2.2 Evaluation of the IR measurements

2.2.1 Evolution of the IR with time

The acquired data set represent several time series stretching over nearly 8 [s], if one machine cycle is measured. The decay constants involved may therefore be evaluated starting within 0.5 [s] after the last extraction. This is novel and opens new ways of looking at beamloss patterns.

If the extraction is followed by a period without beam, the time series may be extended over a long period, depending on the duration of the interval. This is true at least in principle, in practice however, many synchronization events disappear when the beam is stopped, which interrupts most of the 7 measurements.

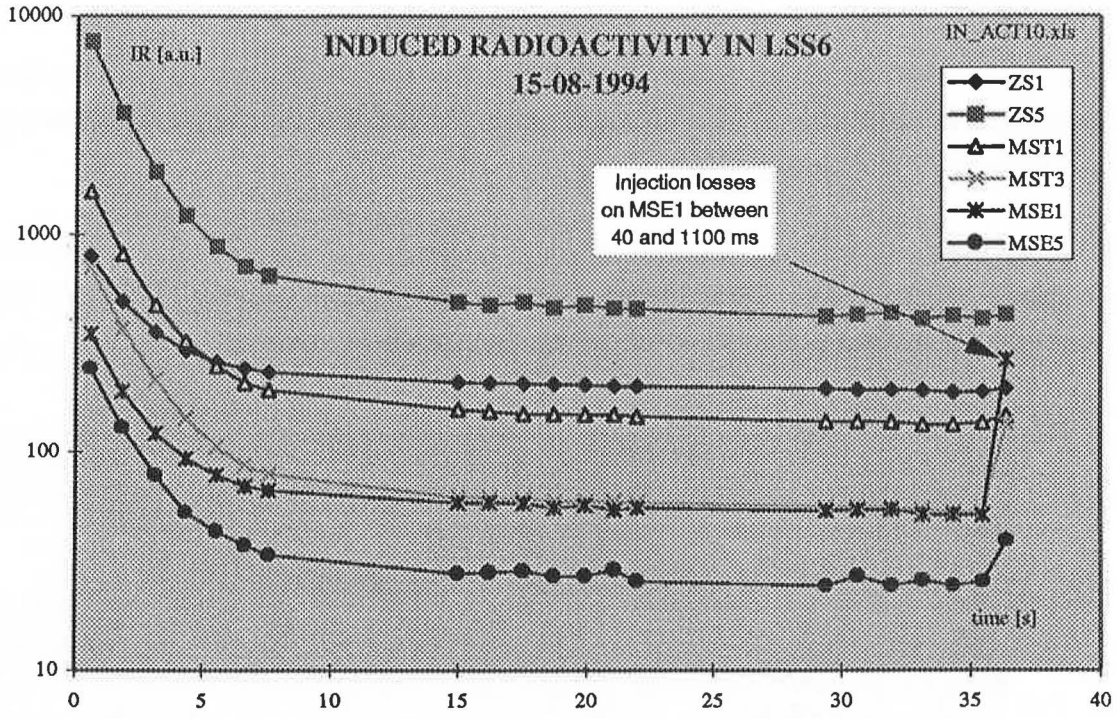

Fig 2 Decay of the IR immediately after f/s extraction

The decay of the IR after the last f/s extraction is shown in fig 2. The exact way the instant of measurement has been obtained is explained in the next two paragraphs.

The active cycle, during which activation took place is followed by three cycles. The first two, 15 to 35 s, are passive and the IR decays. However,

during the third cycle, of which only one point at 36 [s] is shown, the SPS was started-up again. The proton injection losses manifest themselves, mainly on the MST3 and MSE magnets, but also to a lesser degree in the electrostatic septa. Under certain conditions this may cause heavy sparking.

Information about small beam losses during injection or acceleration is a spin-off of the novel technique using high gain amplifiers. The monitors now are used as micro beam loss detectors. The nearly imperceptible increase of the beam loss on the ZS reveals itself only because a time series was measured and by comparison it turns out that one term yields too high a value which can be spotted only by plotting it on a logarithmic scale.

It may also be observed that after the second fast-slow extraction the induced radioactivity decays very rapidly, roughly a factor of 50 from cycle to cycle. Two decay constants manifest themselves, a short and a medium term constant.

The short term decay constant is of the order of 1.8 [s], see fig 3. The first electrostatic septum, ZS1 is less activated than the elements downstream and also decays less rapidly.

The medium term decay constants vary between 20 and 200 [s] depending on the length of the decay period under consideration. Fig 3 shows the analysis for a decay period of 65 [s] or five machine cycles.

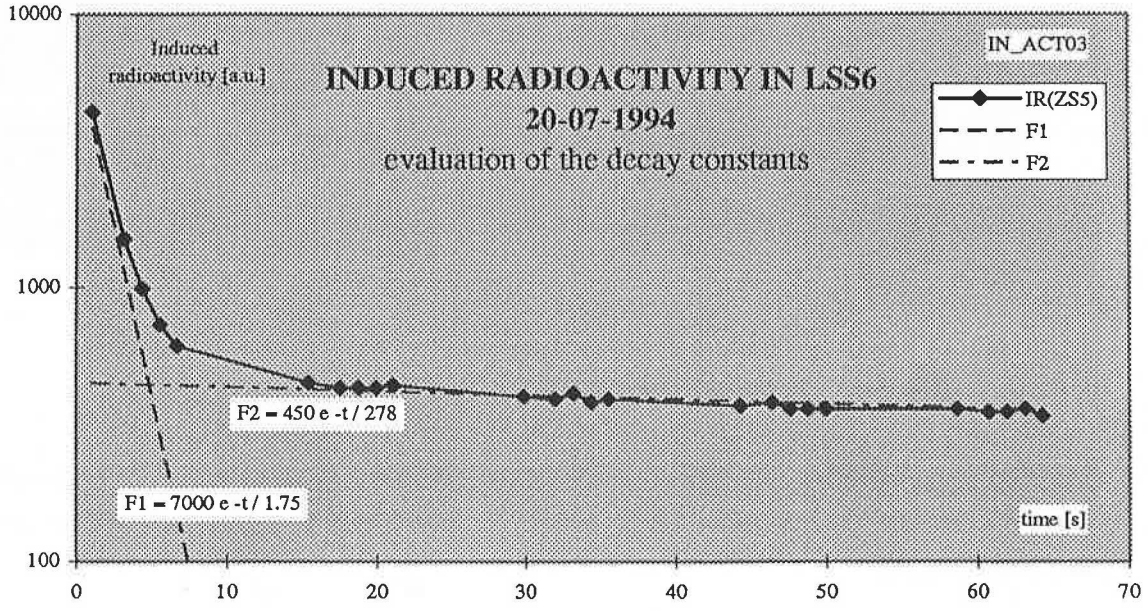

Fig 3 Analysis of the decay of the IR

2.2.2 Calculation of the equivalent acquisition time

For correct display and eventual evaluation of the decay constants it is necessary to know with which exact instant in time corresponds the average value of the IR, measured over a certain period of time.

The average time of the period of measurement cannot be used because of the rapid exponential decay of the IR. Therefore it will be necessary to calculate the average acquisition time by taking this into account.

The extraction in LSS6 consists of a first fast-slow extraction at cycletime 4610 [ms] which is followed by a slow extraction lasting some 2428 [ms]. The second fast-slow extraction is at cycletime 7360 [ms].

Neglecting the slow extraction because of the low intensity, the two fast-slow extractions will generate, at time t, a signal IR(t) consisting of the sum of two components as shown in fig 4 to which a 'constant' IR_L, the remnant induced radioactivity due to elements with long decay constants, should be added.

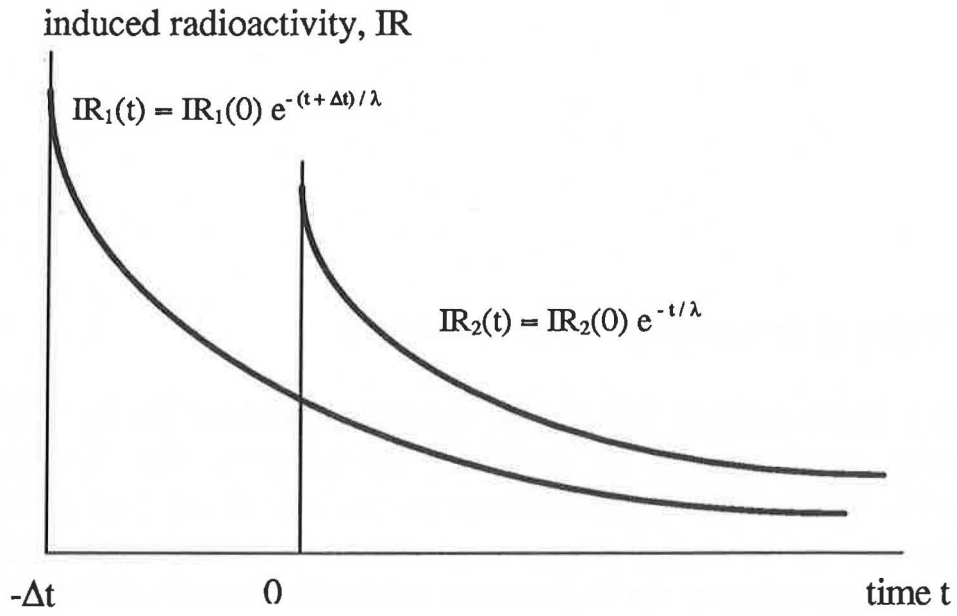

Fig 4 Expected decay of the short term IR

It will be necessary to assume a short time constant λ, for which 1.9 s has been chosen. The exact value is not very important, given the precision of

the measurement, provided that it is short. The expected IR in this case, is given by

$$IR(t) = IR_L + IR_1(0)\, e^{-(t+\Delta t)/\lambda} + IR_2(0)\, e^{-t/\lambda} \qquad (1)$$

where Δt is the delay between the first and the second fast-slow extraction. With $\Delta t = 2.850$ [s], this equation becomes,

$$IR(t) = IR_L + [IR_1(0)\, e^{-2.850/\lambda} + IR_2(0)]\, e^{-t/\lambda} \qquad (2)$$

The amplitudes $IR_1(0)$ and $IR_2(0)$ are proportional to the fast-slow extracted proton intensities. The measured IR then should be analyzed with the function

$$IR(t) = IR_L + IR_{FS}(0)\, e^{-t/\lambda} \qquad (3)$$

where IR_L and $IR_{FS}(0)$ are constants. The first one is the remnant IR which depends on the long term activation and therefore depends on the past history. The second constant is the hypothetical short term amplitude, dependent only on the fast-slow extracted intensities during the current machine cycle.

2.3.3 Table of the equivalent acquisition times

Tables 1 and 3 indicate that the IR signal is integrated during 7 intervals stretching over a period of nearly 8 [s] following the last fast-slow extraction. The measurement evaluates the average IR for each period. The problem now is to calculate the instant t_m when the average value coincides with the exact value of the IR function, with other words, the value of t in expression (3), assuming that the time constant is 1.9 [s].

acquisition	action	start/stop time [s]	interval Δt [s]	eq. acq. time t_e [s]
1	start	7360		
	stop	8629	1260	0.559
2	start	8800		
	stop	9890	890	1.840
3	start	10.150		
	stop	10.890	740	3.148
4	start	11.350		
	stop	12.090	740	4.348
5	start	12.550		
	stop	13.290	740	5.548
6	start	13.750		
	stop	14.340	590	6.677
7	start	40		
	stop	1140	1100	7.604

Table 3 The equivalent acquisition time, t_e

For a specific period lasting Δt [s] the average IR is given by,

$$<IR> = [1/\Delta t] \int [IR_L + IR_{FS}(0)\, e^{-t/1.9}]\, dt \qquad (4)$$

from which follows that,

$$t_e = -1.9 \ln \{1.9/\Delta t * [e^{-t1/1.9} - e^{-t2/1.9}]\} \qquad (5)$$

where t_1 and t_2 represent the beginning and the end of the interval under consideration.

The calculated values are shown in Table 3. It should not be forgotten that the underlying assumption is that the decay constant be 1.9 s which is not exactly the case. However, the error made is much smaller than the precision of the measurement.

2.3 The induced radioactivity

2.3.1 Objectives

The object of this exercise is to answer the following questions:

will it be possible to measure a meaningful induced radioactivity whilst the SPS is running?

in order to obtain reliable long-term values, how long has the SPS to be stopped?

which information is needed to calculate the expected decay curve if the SPS would stop instantaneously, in view of forecasting the waiting time necessary to allow access to the machine tunnel?

2.3.2 Measurement of the induced activity during the SPS supercycle

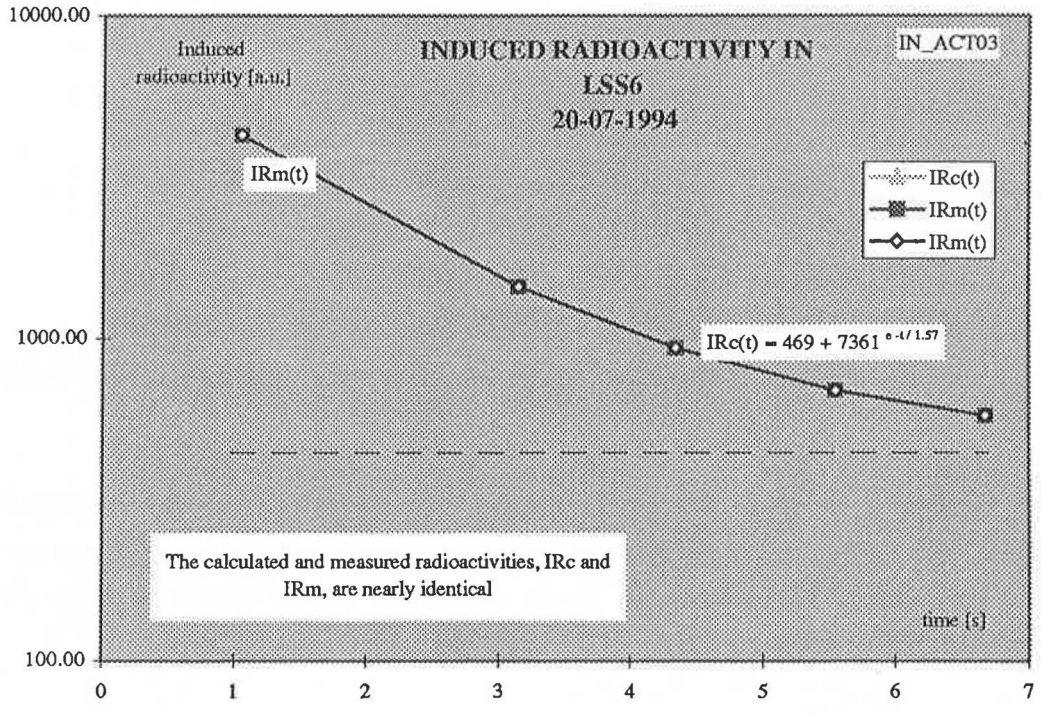

Fig 5 Analysis of the short term decay within the SPS supercycle

The measurement and analysis within one supercycle is shown in fig 5. The calculated and mesured values coincide everywhere. The fitting parameters

have been found by optimization. It turns out that the measured IR approaches an asymptotic value equal to 81% of the last measured value at 6.8 [s], and the short term time constant is 1.57 [s].

However, it is known that the residual radioactivity is not constant but a function containing several decay constants. With this technique a rough estimate of the short term amplitude may be obtained. The latter is a function of the three extracted intensities. However, this does not allow the evaluation of the long term induced activity.

The following graph, fig 6, shows that this short term amplitude is indeed a function of the extracted proton intensities.

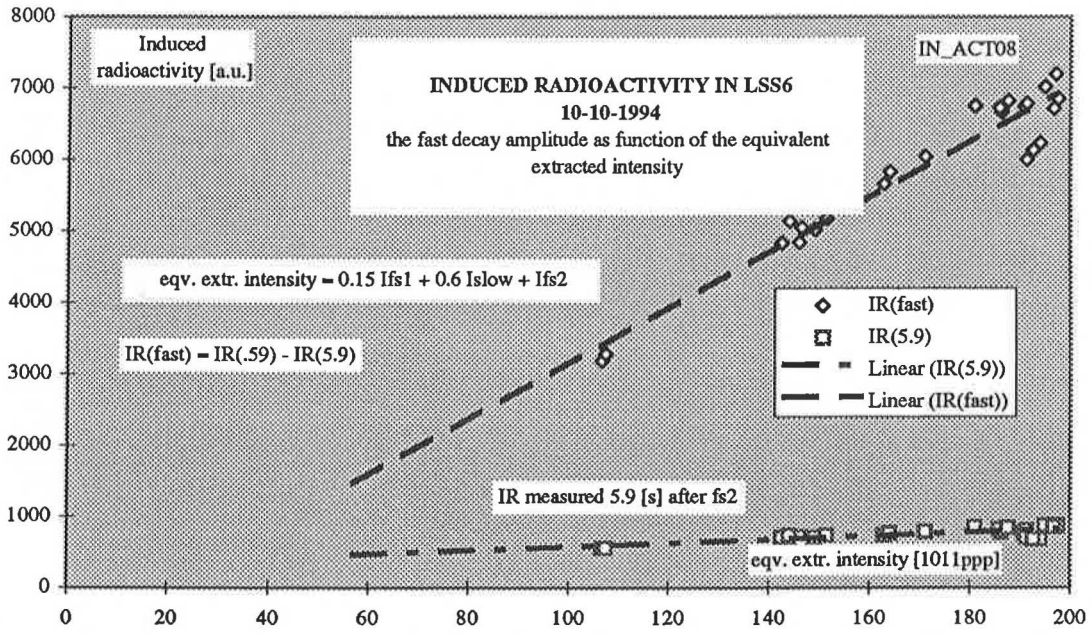

Fig 6 The fast decay amplitude as function of the extracted intensity

For the calculation of the equivalent extracted intensity a short term decay constant of 1.5 [s] has been assumed. The linear dependence of the fast decay amplitude is evident. The long term amplitude is surprisingly constant knowing that this value has been measured only 5.9 [s] after the second fast-slow extraction (fs2).

This graph shows that the long term radioactivity may be calculated by adding algebraically the contribution of each proton extraction. It is not necessary to measure the induced radioactivity but only to monitor the extracted intensities.

The problem is to measure the shape of the decay function IR(t) which contains a great number of decay constants and the equivalence constants which transform extracted intensity into induced radioactivity.

2.4 Evolution of the IR over very long periods

2.4.1 Measurements

The radioactive decay function IR(t) consists of the algebraic sum of a number of exponential functions of which the first two have been described in the previous chapters. A typical analysis is shown in fig 3.

The 1994 proton run was followed by a heavy ion period with no or hardly any excitation of LSS6, allowing the measurement of the 1994 IR decay function. This is specific in the sense that this function is the result of the 1994 proton extraction history. The latter may be defined as the function which describes the evolution with time of the number of protons extracted each day in LSS6.

More precise proton extraction functions could be defined as functions which give the proton extraction history averaged over 75 cycles or the extracted ppp for each supercycle.

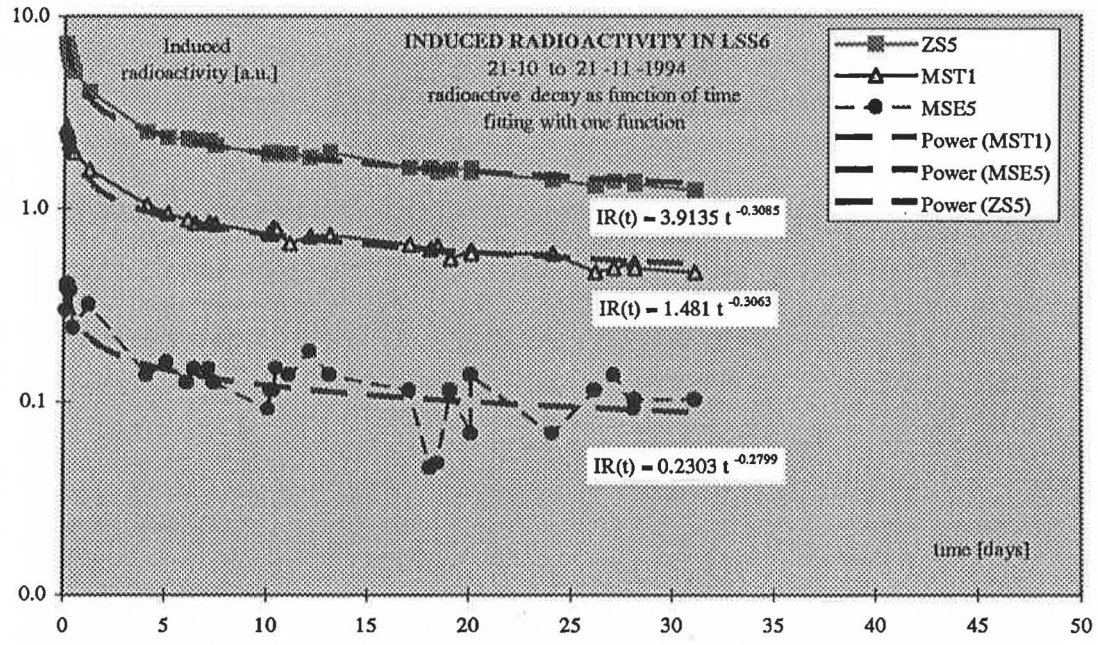

Fig 7 The long term IR decay as function time, fitting with a power function

The long term decay of the LSS6 extraction channel is shown in fig 7. Only ZS5, MST1 and MSE5 are shown for reasons of space but ZS1, MST3 and MSE1 show similar decay curves.

A reasonable fit may be obtained with a power expression of the form

$$IR(t) = IR(0)\, t^{-k} \qquad (6)$$

which does not fit the region between 1 and 5 days very accurately. The power k is roughly 0.3. However the values for t equal to 0 and t equal to infinite are correct.

A much better fit is shown in fig 8. Apparently the decay curves consist of two distinct regions. Region 1 is the period between from 0 to 5 days and Region 2 covers the remaining period from 5 days onwards. For each of these periods a formula of the form

$$IR(t) = k_1 - k_2 \ln t \qquad (7)$$

is valid. The disadvantage is that this formula yields an infinite IR for t equals 0, although fig 8 shows that the fit for t = 0.1 day is still quite good. Furthermore, two sets of constants are needed to cover the whole range and the formula therefore is less suited for computer simulation.

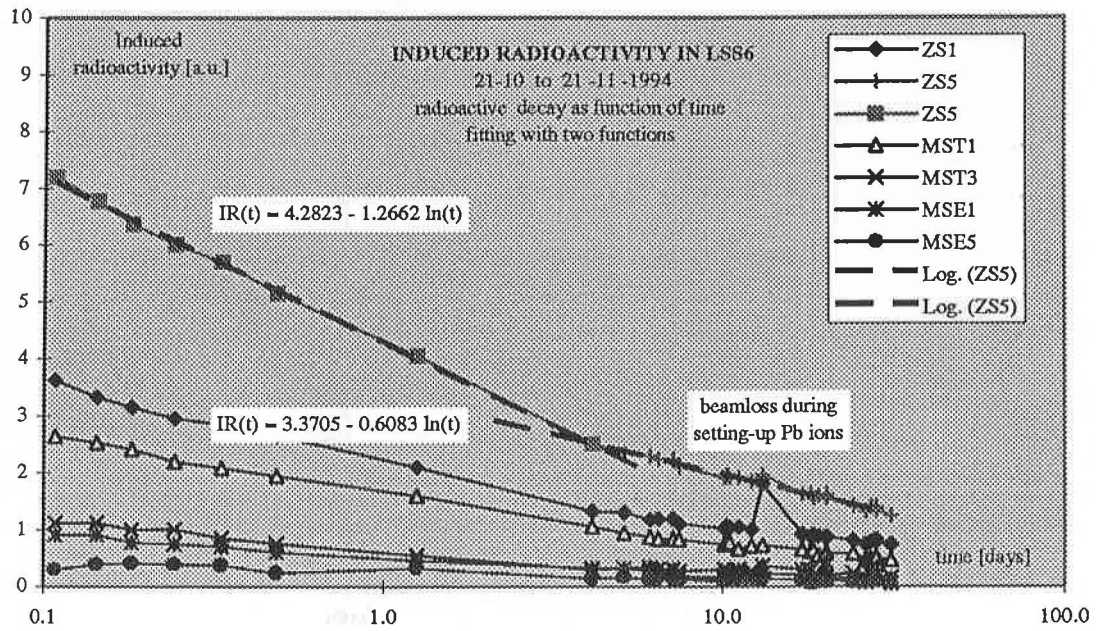

Fig 8 The long term IR decay as function time, fitting with a logarithmic function

The origin of the two expressions in not clear, it could well be that this different behavior is the result of the start-up of the Pb-run, causing nearly imperceptible beam losses, after a stop of 5 days.

A third method is shown in fig 9. A good fit may be obtained with a function of the type

$$IR(t) = IR(0) \exp[- k_1 \ln t - k_2 (\ln t)^2] \qquad (8)$$

This function, for t tending to zero, first reaches a very high maximum and then drops to zero. Nevertheless, this form is very useful and yields a good fit over the whole period under consideration.

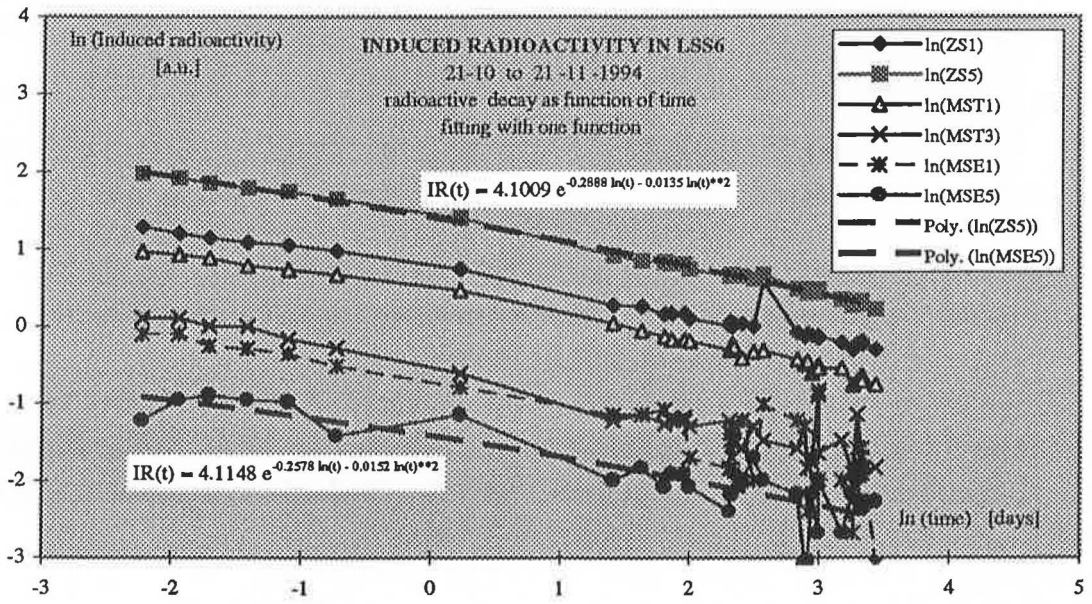

Fig 9 The long term IR decay as function time, fitting with an exponential function

The disadvantage is that there are as many as 3 constants. The first constant IR(0) is related linearly to the time function of the extracted protons P(day). The other two constants k_1, long term, and k_2, short term, have to be determined by curve fitting to measured time function of the induced radioactivity and subsequent measured decay functions.

2.4.2 Evolution of the IR during 1994

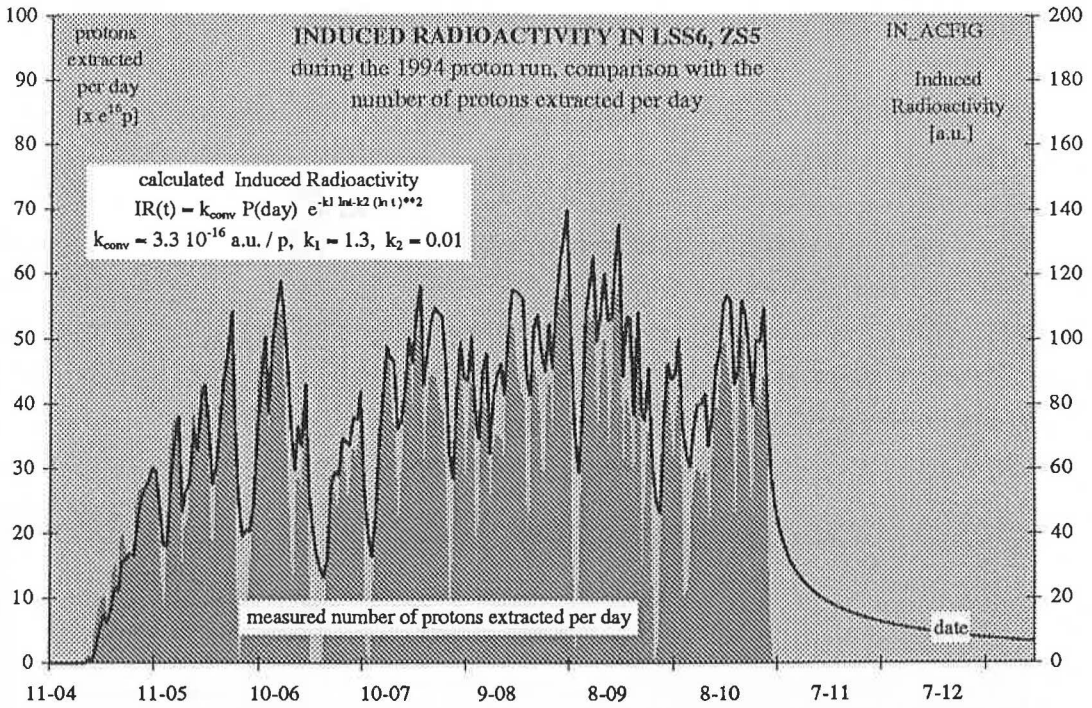

Fig 10 Evolution of the number of protons extracted per day and calculated IR during 1994

The time function of extracted protons in LSS6 during 1994, or the function of the number of protons accelerated per day, P_i(day), was obtained from the SL statistics and is shown shaded in gray in fig 10.

The calculated $IR_j(t)$ function is also shown as a solid line. The expression to calculate the IR contribution to day j by the number of protons, P_i(day), extracted during the day i, is

$$IR_j(t) = k_{conv} P_i(day) \exp[-k_1 \ln t_j - k_2 (\ln t_j)^2] \qquad (9)$$

where the time t_j expressed in days. The time at the end of the first day is assumed to be 1. The partial $IR_j(t)$ caused by the protons extracted at a particular date j is then calculated for each consecutive day. The total IR, the IR(t) function, is then obtained by adding the partial daily contributions. This calculation can readily be done by spreadsheet.

The value of the constants was obtained by fitting this function to the measured IR(t) function as shown in fig 11. The best fit was obtained with

the parameter set: $k_{conv} = 3.33\ 10^{-16}$ arbitrary units of IR per proton extracted, $k_1 = 1.3$ and $k_2 = .01$.

The next problem to be solved will be to calibrate the monitors in mS per hour instead of arbitrary units.

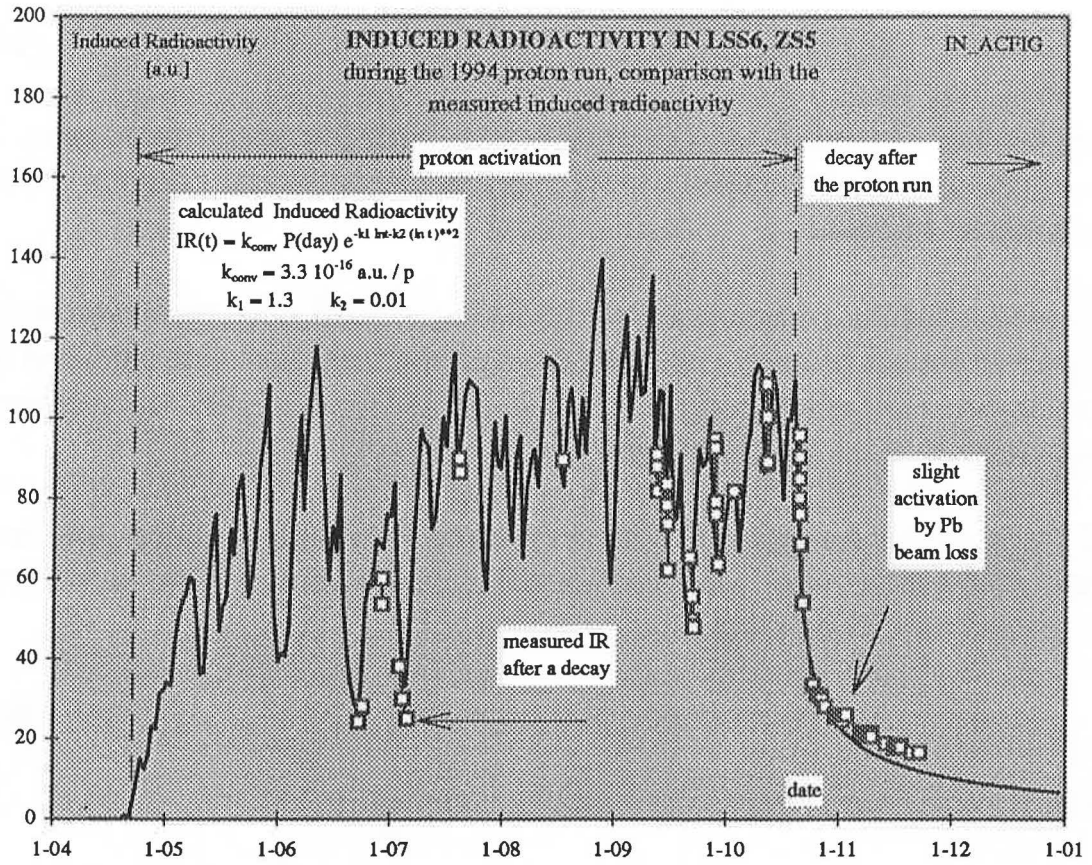

Fig 11 Comparison of the calculated IR during 1994 and measured values

It turns out that, using equation 9 with t set to 1 at the end of the first day, yields an IR(t) function which predicts quite well the radioactivity after a decay of some 4 hours, which is effectively what fig 11 shows. Measurements taken between 5 [s] and a few hours after f/s2 shows values which are two to three times high.

The predicted decay curve during the subsequent Pb-run, assuming no activation, fits reasonably well.

The only aspect which has been neglected in this approach is that zero initial radioactivity has been assumed, which is not strictly the case.

However, because last year's proton run was very similar to this year's, the resulting error is quite small.

2.4.3 Extrapolation to high proton intensities

The expression

$$IR(t) = k_{conv} P(day) \exp[-k_1 \ln t - k_2 (\ln t)^2] \quad (10)$$

allows the evaluation of waiting times for different proton intensities, in particular, what will happen when the proton intensities are doubled as next year could happen.

In section 2.6 the constants $k_1 = 0.28$ and $k_2 = 0.015$ were obtained for the shape of the decay curve after the 1994 proton run. For these values of k_1 and k_2 an expression may be derived for the ratio of the waiting times necessary to reach a certain level of radioactivity.

If for a certain number of extracted protons $P_1(day)$ the waiting time is t_1 days, the waiting time t_2 for a different number of extracted protons $P_2(day)$ is given by the expression

$$t_2 - t_1 [P_2(day) / P_1(day)]^{1/k1} \quad (11)$$

The short term constant k_2 does not appear anymore.

Assuming that $k_1 = 1.3$, which is the value for 1 day of extraction, t_2 will be 1.7 times t_1. The waiting time increases, but less fast than the number of protons extracted. This situation is expected to occur during the setting-up and the first weeks of operation.

Hereafter the situation is expected to worsen progressively, because the long-term decay component of the induced radioactivity will become more and more important. The waiting time will tend to increase.

At the end of next years operation period the situation could be as follows. For $P_2(day)$ equals twice $P_1(day)$, assuming that the constant $k_1 = 0.29$, t_2 will be 12 times t_1. The waiting time increases by a factor of 12. This looks very alarming, given the already important cooling-off time necessary before any intervention can be made for an equipment fault.

3 CALIBRATION OF THE BLX-MONITORS

Two calibrations were carried out. The first one was on 12 October with the SEM electronics and the program described in section 2.1.
The second one took place on 20 October when the IR was a factor of 3 less, with new electronics which was 15.25 times less sensitive and a modified acquisition program. The measured IR values in table 2 have been multiplied by this factor to render the two tables comparable.

12 Oct 1994	ZS1	ZS5	MST1	MST3	MSE1	MSE5
IR [bits/s]	46.0	89.0	39.0	17.0	12.0	6.9
IR_{mon} [mS/h]	20.0	15.0	2.0	1.5	0.9	0.8
cal. factor, C_{mon}	0.43	.17	.05	.09	.07	.12
IR_{tank} [mS/h]	20.0	13.0	3.0	2.0	1.2	1.0
cal. factor, C_{tank}	0.43	.15	.08	.12	.10	.14
IR_{tun} [mS/h]	2.8	3.0	1.2	0.7	0.5	0.4
cal. factor, C_{tun}	.06	.03	.03	.04	.04	.05

Table 4 Calibration of the BLX- monitors on 12 October

20 Oct 1994	ZS1	ZS5	MST1	MST3	MSE1	MSE5
IR [bits/s]	18.2	34.2	12.8	4.7	4.5	2.3
IR_{mon} [mS/h]	7.9	5.0	1.1	.8	.7	.4
cal. factor, C_{mon}	0.44	0.15	0.09	0.16	0.16	0.17
IR_{tank} [mS/h]	10.0	6.4	2.0	1.4	2.0	.9
cal. factor, C_{tank}	0.55	0.19	0.16	0.29	0.44	0.38
IR_{tun} [mS/h]	1.3	1.0	0.5	0.3	0.3	0.1
cal. factor, C_{tun}	0.07	0.03	0.04	0.05	0.06	0.06

Table 5 Calibration of the BLX-monitors on 20 October

With a portable radiation detector the radiation levels were measured on the BLX monitors themselves, on the tank in the median plane and in the tunnel passage. The latter allows a comparison to be made with radioactivity scans carried out by HS-RA during the year.

Tables 4 and 5 show the observed calibration factors. The spread is considerable; ZS1 especially deviates by a factor of 5 from the other monitors. Small differences have been observed during installation. No explanation for this discrepancy has been found and the matter is under investigation.

	ZS1	ZS5	MST1	MST3	MSE1	MSE5
C_{mon}(12 Oct) / C_{mon}(20 Oct)	1.01	0.87	1.69	1.78	2.13	1.46
C_{tank}(12 Oct) / C_{tank}(20 Oct)	1.28	1.28	2.05	2.44	4.57	2.61
C_{tun}(12 Oct) / C_{tun}(20 Oct)	1.19	0.87	1.23	1.27	1.54	1.14

Table 6 Comparison of the two calibrations

The ratio of the calibration factors measured on both occasions is shown in table 6. The ratio should be unity everywhere. However considerable deviations are noticeable. One of the causes is that a great number of similar monitors have been installed. It is easy to measure the wrong one as is apparently is the case with the C_{tank}(12 Oct) / C_{tank}(20 Oct) ratio for MSE1.

All in all one may conclude that the average sensitivity of the BLX monitors is of the order of 0.2 mS/h per bit/s or per a.u.

The maximum dose rate during extraction, see fig 1, is therefore of the order of 200,000 mS/h. Immediately after extraction the level drops to some 2000 mS/h, see fig 2. When the next extraction starts the level is 10 times less.

4 DETECTION OF HOT-SPOTS

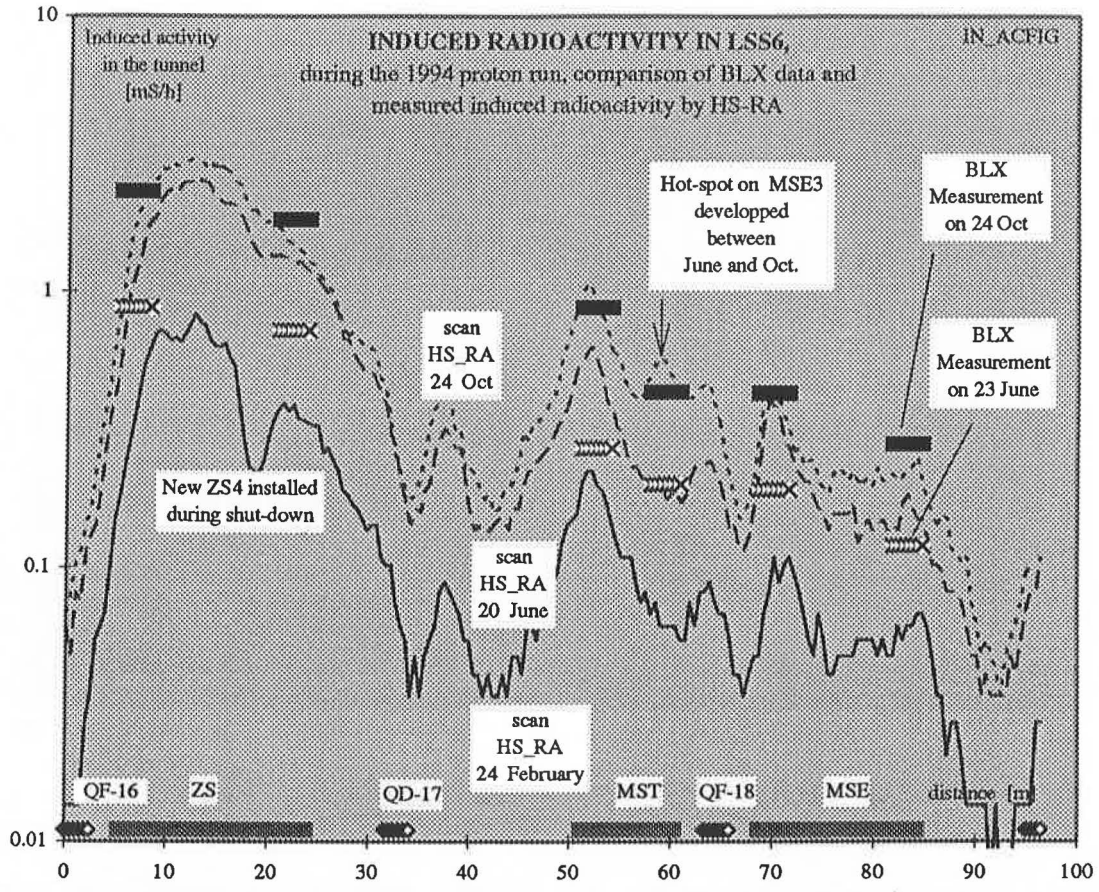

Fig 12 Comparison of the IR scans during 1994 with calibrated BLX measurements

During 1994 the HS_RA group made 3 radioactivity scans in the tunnel of the SPS which are shown in fig 12. The BLX measurements of the 23rd of June do not agree very well with the scan of the 20th of June. However, the end of October observations agree quite well.

Given sufficient number of monitors it is quite well possible to detect hot-spots during operation when the machine is down for a couple of hours.

In order to render the activation of the various elements in the extraction channel visible, the scans of 20 June and 24 October were normalized to the 24 February measurements by calculating the ratio of the activity of corresponding positions. The results are shown in fig 13 for LSS6 and fig 14 for LSS2.

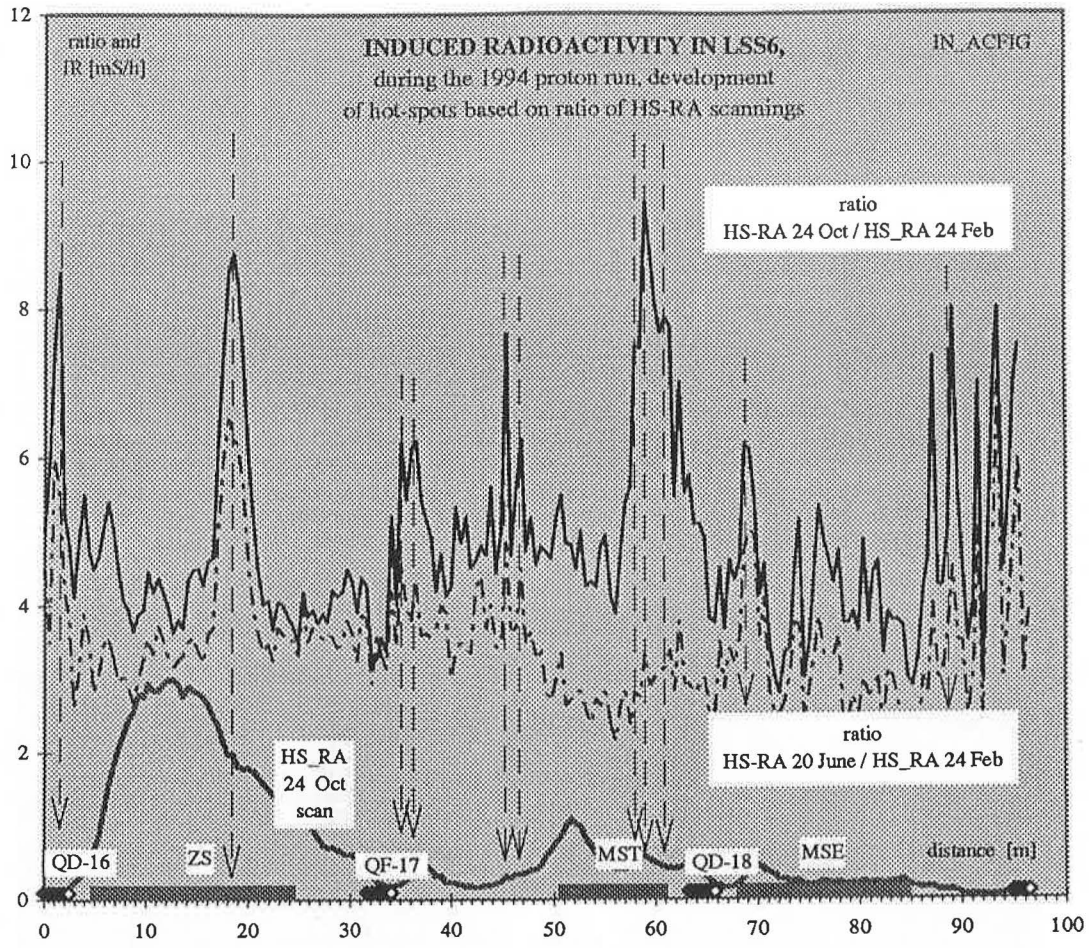

Fig 13 Hot-spots observed in LSS6 during 1994

Fig 13 shows many hot-spots, the average intensity increased by some 400% during the proton run:

QD-16, here the activation is very low and the peak is therefore not very meaningful,

ZS4, this is only an apparent activation, in reality the ZS was replaced during the shut-down and the peak shows a catching-up rather than excessive activation,

QF-17, the correction element after this quad is known to receive much radiation which probably leaks through the TCE,

Position 46 m, also here is a slight activation noticeable,

MST3, this years measurements show a strong activation caused by losses at the end of the ramp sometimes aggravated by injection losses,

MSE1, also activated by losses during ramping,

Position 90m, both in LSS2 and LSS6 some activation took place, the intensities however are very low.

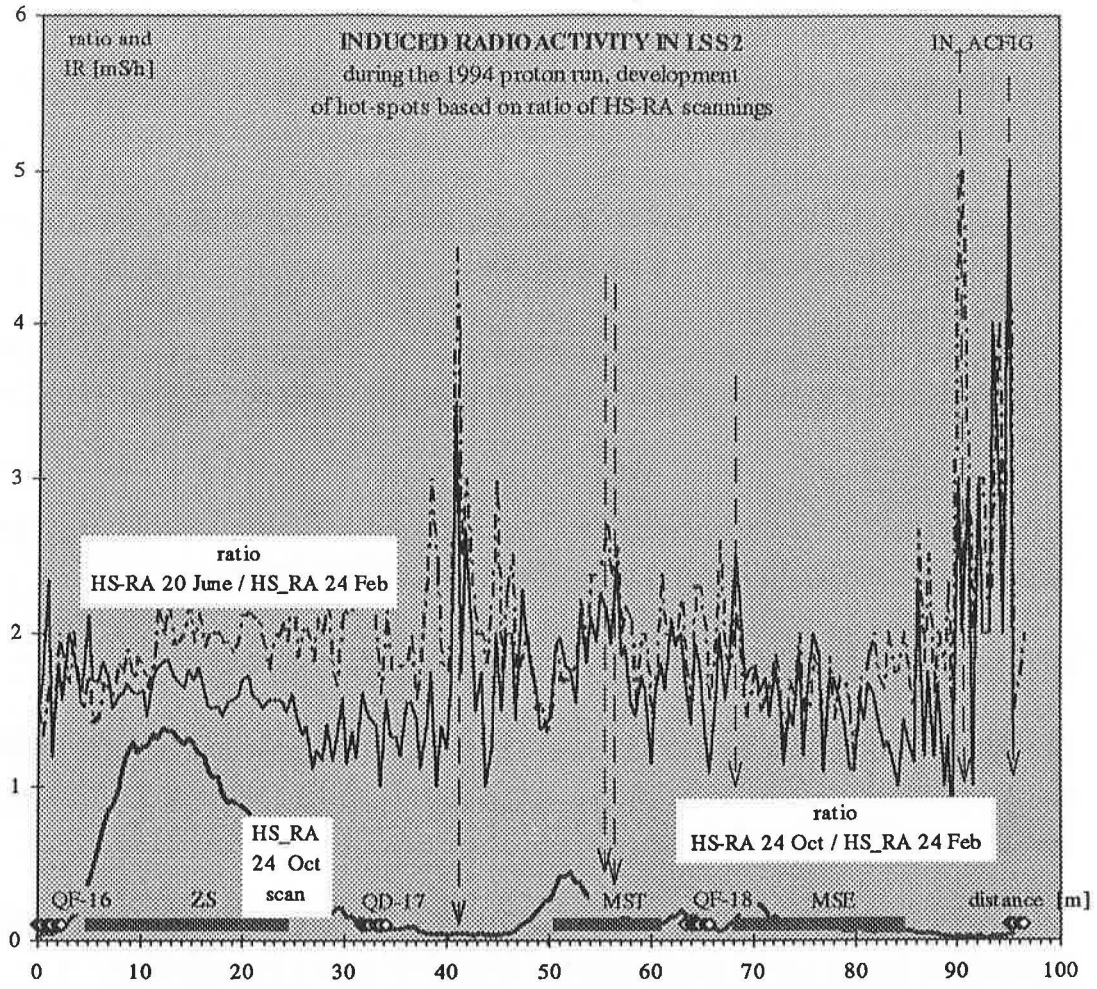

Fig 14 Hot spots observed in LSS2 during 1994

Fig 14 indicates that the radioactivity in LSS2 between June and October diminished. The October activation was only of the order of 50% against 400% in LSS6. There are hardy any hot-spots:

ZS4, no particular activation,

Position 41m, slight activation of an element,

MST2, slight activation, probably also caused by injection problems,

Position 90 m, slight activation as in LSS6.

5 CONCLUSIONS

The measurement of the induced radioactivity in LSS6 during 1994 with six BLX monitors yielded the following results:

radioactive decay curves have been measured between 0.6 [s] to 40 [days] after the second f/s extraction,

the signal strength sometimes increases due to beam loss during proton injection and proton and lepton acceleration; allowance for this should be made,

a by-product is the possibility to measure micro losses during injection and acceleration; this application should be studied further,

the signals from all six monitors decay in a similar manner,

the decay curve consists of a short term amplitude, which decays within a cycletime, and a long term amplitude which becomes a reliable parameter after a few hours,

the short term amplitude is proportional to the locally extracted intensities but as yet is used only for detecting micro beamlosses,

the long term amplitude can be used to detect hot spots, but more monitors are needed for this,

repeated measurements of the long term decay amplitude during 1994 made it possible to evaluate the parameters needed to calculate the expected radioactive decay function of a particular component in the extraction channel from the number of protons extracted per day, refinements of this method are quite possible,

an expression was developed to evaluate the waiting time, leading to an expected factor 12 increase if the number of extracted protons doubled in the future and the incident took place near the end of the p-operation,

attempts have been made to calibrate the monitors in units of mS/hour; the order of magnitude is known but more information is needed.

It is proposed to continue this experiment with 15 BLX monitors in LSS2 and an equal number in LSS2 and to develop a proper database and the necessary applications software to exploit fully the possibility of this new technique.

The expected very long waiting times, before access to the tunnel is possible after periods of successful running, represent a clear warning. The SPS can accelerate high intensities only when the whole accelerator chain works perfectly. All the software necessary to spot instantaneously eventual malfunctioning should be made available and in good working order.

6 ACKNOWLEDGMENTS

The authors would like the thank G Stevenson for his encouragement and assistance in starting a full-size development project after the demonstration was given during the 1993 proton run that the IR measurement was technically feasible.

Distribution :

Altuna X.	SL/OP
Cornelis K.	SL/OP
De Rijk G.	SL/OP
Deluen J.-P.	SL/BT
Faugier A.	SL/OP
Ferioli F.	SL/BI
Ferrari A.	SL/OP
Garrel N.	SL/BT
Goddard B.	SL/BT
Guinand R.	SL/BT
Kalbreier K.	SL/BT
Keizer R.L.	SL/BT
Kissler K.H.	SL/DI
Mertens V.	SL/BT
Stevenson G.R.	TIS/RP
Weisse E.	SL/BT